Turkish Journal of Engineering

FABRICATION OF Cu-Al-Ni SHAPE MEMORY THIN FILM BY THERMAL EVOPRATION

Canan Aksu Canbay *[1], Ayşe Tekataş [2] and İskender Özkul [3]

[1] Fırat University Faculty of Science, Department of Physics, Elazığ, Turkey
(caksu@firat.edu.tr)

[2] Fırat University Faculty of Science, Department of Physics, Elazığ, Turkey
(atekatas@firat.edu.tr)

[3] Mersin University, Engineering Faculty, Department of Mechanical Engineering, Mersin, Turkey
(iskender@mersin.edu.tr)

* Corresponding Author
Received: 13/04/2017   Accepted: 23/05/2017

ABSTRACT

Among the functional, materials shape memory alloys are important because of their unique properties. So, these materials have attracted more attention to be used in micro/nano electronic and electromechanic systems. In this work, thermal evaporation method has been used to produce CuAlNi shape memory alloy thin film. The produced CuAlNi thin film has been characterized and the presence of the martensite phase was investigated and compared with the CuAlNi alloy sample. CuAlNi shape memory alloy thin film about 6.12 µm thick, showing a M→A transformation has been produced and also thermal and structural observations were made to analysis the shape memory behaviour of the Cu-Al-Ni shape memory thin films.

Keywords: Thin films, Shape memory effect, Cu-Al-Ni, Microstructure.

1. INTRODUCTION

Shape memory alloys (SMAs) have attracted considerable interest for mechanical, engineering and medical applications owe to their unique functional properties such as shape memory effect (SME) and superelasticity (SE) (Wang, Zu et al. 2006). SMAs exhibit two different phases, which are called austenite phase and martensite phase. Austenite phase is known as high temperature phase and martensite phase is known as low temperature phase. Austenite and martensite phase start and finish temperatures are named as As, Af, Ms and Mf, respectively (Karagoz and Canbay, 2013). The shape memory effect describes the shape memory via temperature-induced transformation and superelasticity describes the shape memory via stress-induced transformations (Massad and Smith 2005). In some applications both stress and temperature can be affected the transformation of these materials (Recarte, Perez-Landazabal et al. 2004, Lojen, Anžel et al. 2005, Canbay 2010, Izadinia and Dehghani 2011, Kato, Yasuda et al. 2011, Sobrero, La Roca et al. 2012).

SMAs have a diffusionless and first order transformation characterized by an atomic shearing of the crystal lattice from at high temperature to low temperature, which present characteristic structural domains, called martensite variants. Cu-based SMAs show order-disorder phase transitions from high-symmetry crystal structure (at high temperature) to low symmetry crystal structure (at low temperature) (Otsuka and Wayman 1998, Gómez-Cortés, San Juan et al. 2013). Due to the high working capability of SMAs, they have attracted much attention to be used in micro/nano electromechanical systems. So these materials acquired more attention in technological developments. According to this factor, there has been a significant research focused on SMA thin films that could be used in microsystems (Otsuka and Ren 2005).

Thin film fabrication from Cu-Al-Ni SMA has also been the aim of this research. In this work, Cu-Al-Ni thin film produced by thermal evaporation and also thermal and structural observations were made to analysis the shape memory behaviour of the Cu-Al-Ni shape memory thin film. In addition to this, we compare the thermal and structural observation results of the SMA with thin film.

2. EXPERIMENTAL

The sample was prepared from the high purity of Cu (99.9 %), Al (99.9 %) and Ni (99.9 %) elements, and melted in arc melter furnace under vacuum. The obtained sample was cut from the cast ingot, and the specimens were solution-treated at 850 ˚C in β-phase region for 1 h, and then quenched in iced-brine water to obtain the β₁ martensite phase. Then a piece of the homogenized sample was deposited on Si substrate by thermal evaporation method under 4x10-5 T vacuum. The alloy sample and the thin film images are given in Figure 1. For the analysis of alloy sample, the characteristic transformation behaviours were determined with 5, 15, 25 and 35 ˚C/min. heating/cooling rates (Shimadzu DSC-60A differential scanning calorimetry) and for the thermal analysis of the thin film 15 ˚C/min heating/cooling rate was used. The TG/DTA (Shimadzu TA-60 WS) measurements were performed from room temperature to 1000 ˚C at a heating rate of 20 ˚C /min to

identify order-disorder phase transitions at high temperatures. The chemical compositions of the alloy and thin film (Table 1) were examined by Bruker Model energy dispersive X-ray (EDX). X-Ray diffraction patterns of the samples were taken by Rigaku RadB-DMAX II diffractometer. For these examinations, the monochromatic copper Kα radiation with wavelength of 1.5405 Å was used. After the EDX and X-ray analysis, the alloy sample was etched by using a solution consisting of 5g (FeCl3-6H2O)-96 ml methanol with 20ml HCl. The surfaces of the alloy sample and thin film were characterized by Nikon MA200 model optical metallographic microscope. And the thickness of the thin film was observed by scanning electron microscope SEM (LEO evo 40 Model) as 6.12 μm.

Table 1. Chemical compositions of the alloy and thin film (wt. %).

Alloy ID	Cu	Al	Ni
Alloy	82.04	14.60	3.36
Thin film	86.77	11.46	1.77

Fig. 1. The images of Cu-Al-Ni alloy sample and thin film.

3. RESULTS AND DISCUSSION

The alloy sample and the thin film of Cu-Al-Ni were thermally analysed by DSC measurements under nitrogen atmosphere. For the alloy sample 5, 15, 25 ve 35 °C/min. heating/cooling rates were used to determine the austenite→martensite and Fig. 2 illustrates the martensite→austenite phase transitions. DSC studies of the alloy sample have shown that the position of the direct and reverse martensitic transformation peaks remain stable with the thermal cycling occurred during the measurement of the different heating rates. And also the hysteresis observed from the DSC analysis, is one of the typical characteristics of the thermoelastic martensitic transformations. During this transformation, nucleation process occurred rapidly and the activation energy of this transformation is very small (Canbay 2010, Karagoz and Canbay 2013). The characteristic transformation temperatures of high temperature phase and low temperature phase such as As, Af, Ms and Mf of the samples are determined, where the DSC curve deviates from linearity. The obtained results from the DSC measurements for the alloy sample are given in Table 2. When we compare the characteristic transformation temperatures of fabricated Cu-14.6 Al-3.36 Ni (% wt.) with the Cu-14 Al-4 Ni (% wt.), Cu-13.3 Al-4.0 Ni (%

wt.) and Cu-13 Al-4 Ni (% wt.), the transformation temperatures of the investigated alloy is low. On the other hand, according to Cu-13.5 Al-4 Ni (% wt.) and Cu-13.83 Al-2.34 Ni (% wt.) the transformation temperatures of the investigated alloy is high. As a result of this, we can assume that in Cu-Al-Ni system aluminium is also affected the characteristic transformation temperatures and especially aluminium is more effective then copper in binary Cu-Al system. So, the aluminium is dominant on the characteristic transformation temperatures in Cu-Al-Ni system then nickel. The change in Af-Ms hysteresis is shown in Fig. 3 and the hysteresis increases with the increase of the heating/cooling rate. This is a well-known situation in SMA systems, that the increase of heating/cooling rate also effects the transformation temperatures (Canbay 2010).
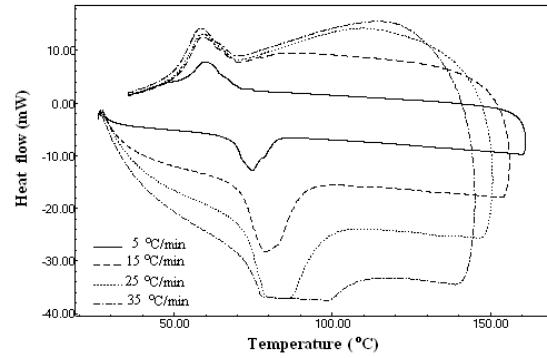

Fig. 2. DSC curves of Cu-Al-Ni alloy sample with 5, 15, 25, 35 ˚C/min. heating/cooling rates.

Table 2. Characteristic transformation temperatures and thermodynamic parameters of Cu-Al-Ni alloy.

Heating/cooling rate (˚C/min.)	As (˚C)	Af (˚C)	Amax (˚C)	Ms (˚C)	Mf (˚C)	Mmax (˚C)	ΔHM→A (J/g)	ΔHA→M (J/g)
5	68,47	82,38	74,70	66,90	54,45	60,27	-8,19	8,69
15	71,36	90,29	79,05	70,88	40,06	58,97	-9,69	5,01
25	72,17	96,10	86,35	68,75	51,52	58,60	-8,99	5,65
35	59,16	118,83	90,16	69,84	45,07	58,33	-5,18	5,83

The absorbed and released energy during heating and cooling related to the enthalpy values of austenite and martensite phases. So the energy required for the low temperature (martensite phase) and high temperature (austenite phase) transitions varied with the variation of the heating and cooling rates. As seen in Fig. 4 and Fig. 5 the enthalpy change during heating and cooling is given for the alloy sample. For the thin film, we cannot detect enthalpy values according to different heating and cooling rates.
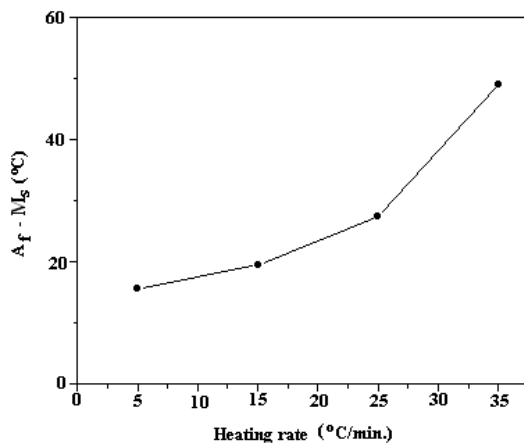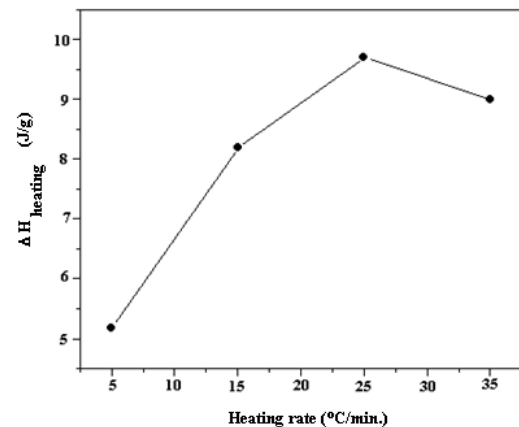

Fig. 4. The variation of enthalpy during heating (ΔHheating) versus heating/cooling rate.
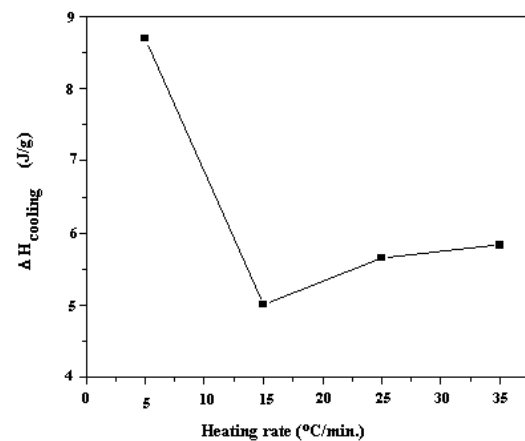
Fig. 5. The variation of enthalpy during cooling (ΔHcooling) versus heating/cooling rate.

Fig. 3. The variation of (As-Ms) hysteresis versus heating/cooling rate.

The activation energy values according to Kissinger and Ozawa methods are calculated to determine the kinetic parameters of the alloy sample. The activation energy value processed with the following equation developed by Kissinger (Kissinger 1957):

$$\frac{d\left[\ln\left(\phi/T_m^2\right)\right]}{d\left(1/T\right)} = -E/R \tag{1}$$

where ϕ is the heating rate, T_m is the maximum temperature of the DSC peak, R is the universal gas constant, and E is the activation energy and according to Ozawa (1970):

$$E = \frac{-R}{b}\left[\frac{d(\log\phi)}{d\left(1/T_m\right)}\right] \tag{2}$$

where b is a constant (0.4567).The activation energy values were calculated for the reverse transformation according to Kissinger and Ozawa methods and are 116,48 kJ/mol and 116,33kJ/mol, respectively. When we compare the activation energy values of the alloy sample according to the Kissinger and Ozawa methods independently, the values of both methods are the same. The activation energy of the thin film was not determined because only one heating/cooling rate can be used for the thermal analysis.
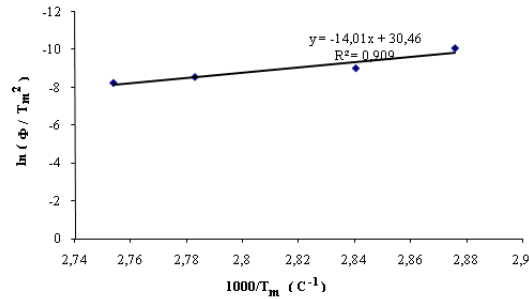
(a)
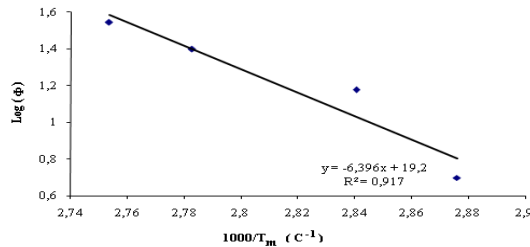
(b)

Fig. 6. Activation energy curves of the alloy sample; a) Kissinger, b) Ozawa methods.

The DSC curve of the thin film is given in Fig.7. As seen from the figure only martensite→austenite phase transition was observed and the reverse transformation was not detected. This is mainly due to the low weight percentage of the thin film put into pans for the thermal analysis. Because it is well known that appropriate alloy concentration is required for a good shape memory effect. But for the thermal analysis of the thin film, it is evident that the appropriate alloy concentration is not been provided so we can only observed A→M phase transition. In addition to this, only one heating/cooling rate was used to determine the phase transition of the thin film and the thermodynamic parameters obtained from the thermal analysis is given in Table 3.
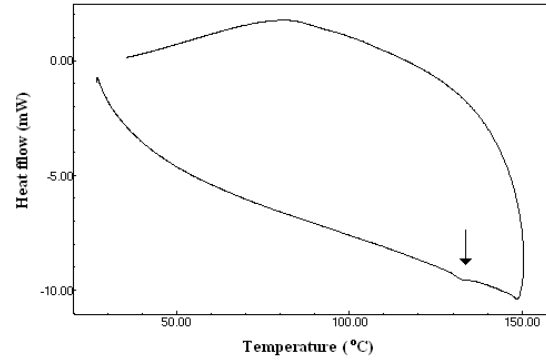

Fig. 7. DSC curve of the thin film. with a heating/cooling rate of 15 ˚C/min.

Table 3. Characteristic transformation temperatures and thermodynamic parameters of thin film.

Heating/cooling rate (˚C/min.)	A_s (˚C)	A_f (˚C)	A_{max} (˚C)	$\Delta H_{M\to A}$ (J/g)
15	129,10	141,34	122,95	-0,56

The diffraction patterns of the alloy sample and thin film are given in Fig. 8. The main peak of the martensite phase, which was observed in both alloy and thin film is (0018). And (0018) plane is one of the main phase of martensite at room temperature. An interesting observation in XRD patterns, is the peaks laid between $2\theta=35˚$ to $45˚$ that represented martensite structures formed. These planes have monoclinic crystal symmetry and the lattice parameters are a=4.420 Å b=5.260 Å and c=37.89 Å. The calculated a/b ratio is 0.84 and this value is smaller than $\sqrt{3}/2$. This indicates that, the main phase of the alloy and thin film is ordered and the atoms in the planes are in different sizes (Xuan, Bohong et al. 1987, Pérez-Landazábal, Recarte et al. 2006, Meng, Yang et al. 2010). The diffraction planes of the observed alloy sample and the thin film is the generally observed peaks in Cu-Al-Ni shape memory alloys and belong to M18R structure (Xuan, Bohong et al. 1987, Canbay 2010, Meng, Yang et al. 2010).

The average crystallite size (D) for the alloy and thin film was determined by Debye-Scherrer equation (Izadinia and Dehghani, 2011).

$$D = \frac{0.9\lambda}{B_{1/2}\cos\theta} \tag{3}$$

where λ is the wavelength of the X-ray (CuK$_\alpha$ radiation), B is the peak full width at half maximum and θ is the Bragg angle. The calculated crystallite size of the alloy is

19.57 nm and the thin film is 12.37 nm. The optical microscopy observations of the alloy (Fig. 9) revealed that, the parent phase has martensite structure at room temperature. The martensite variants and the grain boundaries in the CuAlNi alloy sample are clear. In Figure 9.b, the surface of the thin film is given. The surface of the thin film is smooth, and there is no martensite variants observed at room temperature.
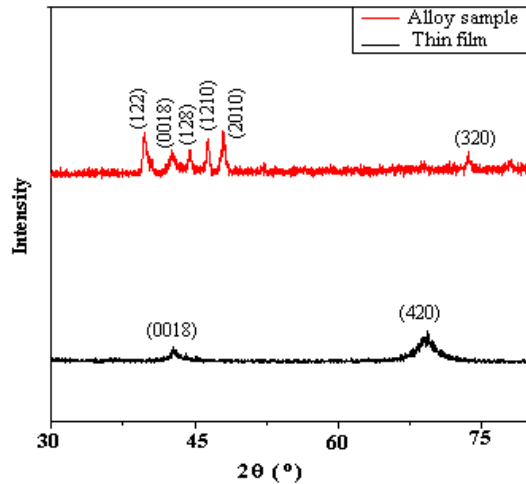

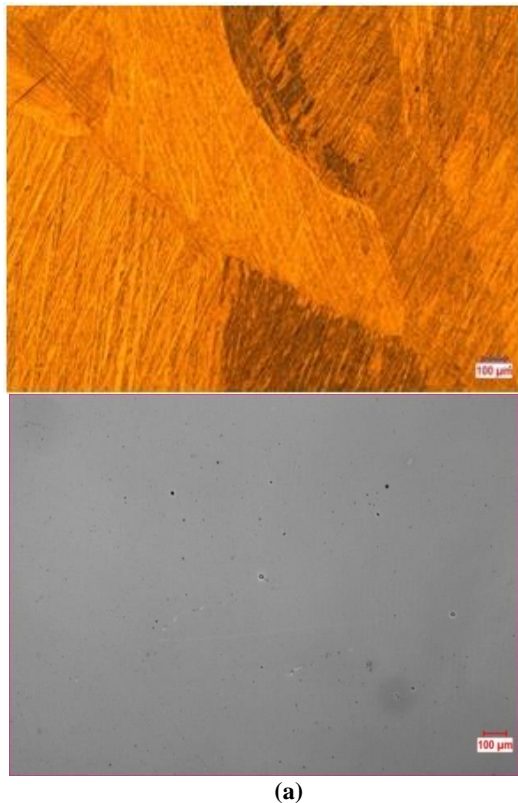Fig. 8. X-Ray diffraction patterns of the alloy and thin film.

(a)

Fig. 9. Optical micrographs of a) alloy and b) thin film.

4. CONLUSION

The thermodynamical and structural properties of CuAlNi alloy and thin film were investigated. The thermoelastic phase transformations at the ternary CuAlNi SMA system and thin film were observed by heating- cooling processes with DSC analysis. Furthermore, by using different heating and cooling rates to the CuAlNi ternary alloy system, obtained characteristic transformation temperatures and enthalpy values have been found to be changing. The hysteresis value of Af-Ms increased by the increase of heating/cooling rate and the enthalpy changed with the variation of the heating/cooling rate. For the thin film, only M→A transformation was observed and this observation can be detected only one heating/cooling rate. The XRD analysis of the CuAlNi alloy and thin film showed that both of the samples have martensitic structure at room temperature. And this was confirmed with the optical microscope observations for the CuAlNi alloy but we cannot detect any martensitic variants for the thin film.

REFERENCES

Canbay, C. A. (2010). The production of Cu-based shape memory alloys and investigation of microstructural, thermal and electrical properties of alloys, Ph. D Thesis, Fırat University, Institute of Science, Elazığ/Turkey (Turkish).

Gómez-Cortés, J., J. San Juan, G. López and M. Nó (2013). "Synthesis and characterization of Cu–Al–Ni shape memory alloy multilayer thin films." *Thin Solid Films* Vol. 544, No. pp. 588-592.

Izadinia, M. and K. Dehghani (2011). "Structure and properties of nanostructured Cu-13.2 Al-5.1 Ni shape memory alloy produced by melt spinning." *Transactions of Nonferrous Metals Society of China* Vol. 21, No. 9 pp. 2037-2043.

Karagoz, Z. and C. A. Canbay (2013). "Relationship between transformation temperatures and alloying elements in Cu–Al–Ni shape memory alloys." *Journal of Thermal Analysis and Calorimetry* Vol. 114, No. 3 pp. 1069-1074.

Kato, H., Y. Yasuda and K. Sasaki (2011). "Thermodynamic assessment of the stabilization effect in deformed shape memory alloy martensite." *Acta Materialia* Vol. 59, No. 10 pp. 3955-3964.

Kissinger, H. E. (1957), "Reaction kinetics in differential thermal analysis." *Analytical chemistry* Vol. 29, No. 11 pp. 1702-1706.

Lojen, G., I. Anžel, A. Kneissl, A. Križman, E. Unterweger, B. Kosec and M. Bizjak (2005).

"Microstructure of rapidly solidified Cu–Al–Ni shape memory alloy ribbons." *Journal of Materials Processing Technology* Vol. 162, No. pp. 220-229.

Massad, J. E. and R. C. Smith (2005). "A homogenized free energy model for hysteresis in thin-film shape memory alloys." *Thin Solid Films* Vol. 489, No. 1 pp. 266-290.

Meng, Q., H. Yang, Y. Liu and T.-h. Nam (2010). "Transformation intervals and elastic strain energies of B2-B19 ′ martensitic transformation of NiTi." *Intermetallics* Vol. 18, No. 12 pp. 2431-2434.

Otsuka, K. and X. Ren (2005). "Physical metallurgy of Ti–Ni-based shape memory alloys." *Progress in materials science* Vol. 50, No. 5 pp. 511-678.

Otsuka, K. and C. Wayman (1998). "Mechanism of shape memory effect and superelasticity." *Shape memory materials*, No. pp. 27-48.

Ozawa, T. (1970). "Kinetic analysis of derivative curves in thermal analysis." *Journal of Thermal Analysis and Calorimetry* Vol. 2, No. 3 pp. 301-324.

Pérez-Landazábal, J. I., V. Recarte, V. Sánchez-Alarcos, M. L. Nó and J. S. Juan (2006). "Study of the stability and decomposition process of the β phase in Cu–Al–Ni shape memory alloys." *Materials Science and Engineering: A* Vol. 438–440, No. pp. 734-737.

Recarte, V., J. Perez-Landazabal, P. Rodrıguez, E. Bocanegra, M. No and J. San Juan (2004). "Thermodynamics of thermally induced martensitic transformations in Cu–Al–Ni shape memory alloys." *Acta materialia* Vol. 52, No. 13 pp. 3941-3948.

Sobrero, C., P. La Roca, A. Roatta, R. Bolmaro and J. Malarría (2012). "Shape memory properties of highly textured Cu–Al–Ni–(Ti) alloys." *Materials Science and Engineering: A* Vol. 536, No. pp. 207-215.

Wang, Z., X. Zu, H. Yu, X. He, C. Peng and Y. Huo (2006). "Temperature memory effect in CuAlNi single crystalline and CuZnAl polycrystalline shape memory alloys." *Thermochimica acta* Vol. 448, No. 1 pp. 69-72.

Xuan, Q., J. Bohong, T. Hsu and X. Zuyao (1987). "The effect of martensite ordering on shape memory effect in a copper-zinc-aluminium alloy." *Materials Science and Engineering* Vol. 93, No. pp. 205-211.